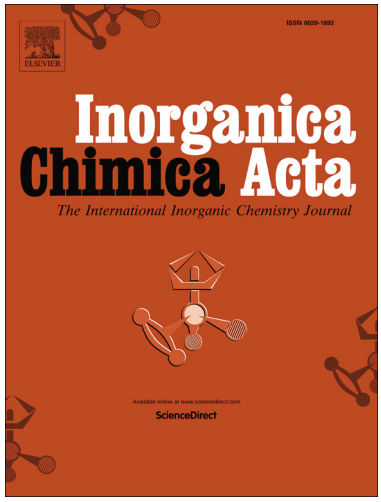

Research paper

Photoluminescence and electrochemical studies of tetranuclear ruthenium(II) polypyridyl complexes of benzimidazolyl functionalised pyrenylcalixresorcinarene

Ligimol Louis, V. Alexander, D. Suresh Kumar, S. Amudhan Senthan, A. Arun Viveked

PII: S0020-1693(18)31040-5
DOI: https://doi.org/10.1016/j.ica.2018.10.043
Reference: ICA 18589

To appear in: *Inorganica Chimica Acta*

Received Date: 7 July 2018
Revised Date: 21 October 2018
Accepted Date: 21 October 2018

Please cite this article as: L. Louis, V. Alexander, D.S. Kumar, S.A. Senthan, A.A. Viveked, Photoluminescence and electrochemical studies of tetranuclear ruthenium(II) polypyridyl complexes of benzimidazolyl functionalised pyrenylcalixresorcinarene, *Inorganica Chimica Acta* (2018), doi: https://doi.org/10.1016/j.ica.2018.10.043

Photoluminescence and electrochemical studies of tetranuclear ruthenium(II) polypyridyl complexes of benzimidazolyl functionalised pyrenylcalix[4]resorcinarene

Ligimol Louis[a], V. Alexander[b], D. Suresh Kumar[a]*, S. Amudhan Senthan[c], A. Arun Viveke[d]

[a] *Supramolecular Research Lab, Department of Chemistry, Loyola College, Chennai-600034, India*

[b] *Department of Chemistry, Loyola College, Chennai-600034, India*

[c] *Department of Chemistry, Pondicherry University, Puducherry-605014, India*

[d] *Department of Chemistry, St. Joseph's College, Tiruchirappalli-620002, India*

** Corresponding author, drdsk24@gmail.com.*

Abstract

We report the hitherto unreported pyrene footed calix[4]resorcinarene (**P1**) supramolecular assembly and its tetranuclear Ru(II) polypyridyl complexes, $[\{Ru(phen)_2\}_4(\mathbf{L})](ClO_4)_8$ (**CP1**), $[\{Ru(bpy)_2\}_4(\mathbf{L})](ClO_4)_8$ (**CP2**), and $[\{Ru(\mathbf{P2})_2\}_4(\mathbf{L})](ClO_4)_8$ (**CP3**) [where, **L** = 2,8,14,20-Tetra(pyren-1-yl)-5,11,17,23-tetrakis((2-(pyridin-2-yl)-1*H*-benzimidazol-1-yl)methyl)-4,6,10,12,16,18,22,24-octahydroxy-calix[4]resorcinarene and **P2** = 2-(pyridin-2-yl)-1*H*-benzimidazole]. The single crystal structure of 2,8,14,20-tetra(pyren-1-yl)-4,6,10,12,16,18,22,24-octahydroxycalix[4]-resorcinarene (**P1**) possesses all *cis* configuration and a boat like conformation with pyrene rings occupying the axial positions. The tetranuclear complexes, **CP1**, **CP2** and **CP3**, show decreasing energy of ^{3}MLCT luminescence at 298 K but the intensity is increased at 77 K in frozen acetonitrile due to lowering of energy gap between π^* of the ligand and the d orbital of ruthenium metal ion. The luminescence quantum yield has also been increased considerably in all the complexes when the temperature is decreased from 298 K to 77 K due to combined restricted rotations of pyrene groups in the ligand and as well that of ancillary ligands, which enhance luminescence emission. The complexes exhibit a single exponential decay profile in acetonitrile at 298 K. The cyclic voltammograms of the complexes show simultaneous four single electron quasireversible redox processes.

Key Words: Pyrenylresorcinarene, Ruthenium(II) complex, Luminescence, Pyridinyl benzimidazole, Crystal structure.

1. Introduction

Calix[4]resorcinarene, a unique three dimensional cyclic aromatic tetramer and an important building block for supramolecular compounds, draw constant attention of chemists for producing new functional supramolecules with its versatile receptor properties [1]. They are intrinsically interesting due to their complexing abilities, conformational flexibility, reactivity, high polarity, and the bowl shape [2]. Calix[4]resorcinarenes form a variety of complexes with organic or inorganic ions, neutral molecules and transition metal ions [3]. Introduction of relatively rigid aryl groups on calix[4]resorcinarene makes it to attain more stable conformation [4]. The two activating hydroxyl groups make the '*ortho'* position of the calix[4]resorcinarene electron rich and thus suitable for electrophilic substitutions [2,5]. The ruthenium polypyridyl complexes when appended on to the ortho position of resorcinarene will modify the photophysical, and electrochemical properties of calix[4]resorcinarenes [6]. Also the pyrene ring in conjugation with the resorcinarene affects the photophysical properties of ligand or metal ion to a considerable extent [7]. Herein we put forth an efficient method to synthesize benzimidazolyl functionalized calix[4]resorcinarene ligand and its ruthenium(II) complexes to probe their electrochemical and temperature dependent photophysical properties.

2 Experimental Section

2.1 Materials and physical measurements

All reagents were commercially available and used without further purification. The solvents were purified by the standard procedures. ^{1}H NMR spectra were recorded on a Bruker Avance III 500 MHz spectrometer. Microanalysis (C, H, and N) were carried out using a Perkin-Elmer 2400 Series II CHNS/O Elemental Analyzer. The electrospray mass spectra were recorded on a Micromass Quattro II triple quadrupole mass spectrometer. UV-Visible spectra were recorded on a Shimadzu UV-2450 UV-Visible spectrophotometer and the fluorescence spectra were recorded on a Fluorolog-3 FL3-221 spectrofluorometer. Experiments at 77 K in acetonitrile were carried out in frozen glasses made up of quartz capillary tubes immersed in liquid nitrogen contained in a quartz dewar. The emission lifetimes were measured using nanosecond laser flash photolysis. Emission quantum yields (Φ) were calculated by integrating the area under the luminescence curves by using Eq. 1 [8] where OD is optical density of the compound at the excitation wavelength and A is the area under the emission spectral

curve. The standard used for the luminescence quantum yield measurements was $[Ru(bpy)_3]Cl_2$ (Φ = 0.04) [9] and corrected for the refractive index (η) of the solvent.

$\Phi_{sample} = (OD_{std}A_{sample}\eta^2_{sample}/OD_{sample}A_{std}\eta^2_{std})\Phi_{std}$ **Eq. 1**

Cyclic voltammetry was performed on a EG&G PAR 273A Potentiostat/Galvanostat using RDE0018 Analytical Cell Kit consisting of a thermostated cell bottom, EG&G G0229 glassy carbon disk milli-electrode, platinum counter electrode, and EG&G K0265 Ag/Ag^+ reference electrode. Single crystal X-ray structure data collections were performed on a Bruker AXS Kappa Apex II CCD diffractometer using graphite monochromatic Mo (K_α) radiation (λ = 0.71073 Å). The structures were solved by direct methods using SHELX-97, and successive Fourier synthesis was employed to complete the structures after full-matrix least squares refinement on $|F|^2$ using the SHELXL-2014/7.

2.2 Synthesis of pyrenylcalix[4]resorcinarene (P1)

To an ethanolic solution (35 mL) of resorcinol (1.10 g, 10 mmol), conc. hydrochloric acid (10 mL) was added, mixed well and then diluted with water (35 mL). It was then stirred at 70 °C for 1 h under argon atmosphere. A solution of 1-pyrenecarboxaldehyde (2.30 g, 10 mmol) in ethanol (50 mL) was added to the above reaction mixture and refluxed for 100 h. The resulting suspension was cooled to room temperature, filtered through a G4 filter funnel, washed and dried under vacuum to obtain a brown powder. The solid product was purified using column chromatography by eluting with ethyl acetate-hexane (2:1 v/v) solvent mixture and recrystallized using dimethyl formamide (DMF) to get brown crystals suitable for X-ray diffraction analysis. **P1** – Brown crystal (10.45 g, 81 %), mp >300 °C (dec.). Analytical data (%) found: C, 85.76; H, 4.44; calculated for $C_{92}H_{56}O_8$: C, 85.70; H, 4.38. ^{1}H NMR data (500 MHz, DMSO-d_6, 298 K) δ 5.90 (4H, s, -CH-), 6.10 (2H, s), 6.39 (4H, d), 6.49 (2H, s) 6.71 (4H, s), 6.81 (4H, s), 7.01 (4H, d), 7.28 (4H, s), 7.52 (4H, m), 7.69 (4H, m) 7.85 (4H, t), 8.06 (4H, d), 8.40 (4H, d) 9.01 (8H, -OH) ^{13}C NMR data (125 MHz, DMSO-d_6, 298 K) δ 19.03, 102.74, 120.68, 121.05, 123.47, 123.87, 124.19, 124.71, 125.72, 125.94, 126.32, 126.92, 127.72, 128.42, 129.73, 130.91, 139.18, 152.42, 153.29. ESI-TOF MS: m/z 1289 $[M]^+$, 1312 $[M + Na]^+$.

2.3 Synthesis of 2-(pyridin-2-yl)-1*H*-benzimidazole (P2)

2-(Pyridine-2-yl)-1*H*-benzimidazole was prepared by the modification of the procedure reported by Addison [10] by using cyanopyridine instead of 2-

pyridylaldehyde or pyridine-2-caboxylic acid. 2-Cyanopyridine (9.6 mL, 100 mmol) and 60 mL of *o*-phosphoric acid were stirred for one hour in 250 mL single neck round bottom flask. To this pink solution, a solution of *o*-phenylene diamine (10.81 g, 100 mmol) was added and the reaction mixture was refluxed for 24 h. It was then cooled to room temperature, poured into 600 mL ice cubes and neutralised with aq. ammonia. The pink precipitate that separated out was filtered, washed, dried and recrystallized in hot methanol. **P2** – Pink crystal (17 g, 87%), mp 220 °C. Analytical data (%) found: C, 73.90; H, 4.72; N, 21.59; calculated for $C_{12}H_9N_3$: C, 73.83; H, 4.65; N, 21.52. ^{1}H NMR data (500 MHz, DMSO-d_6, 298 K) δ 7.23 (2H, m), 7.52 (2H, m), 7.71 (1H, d), 8.00 (1H, t), 8.33 (1H, d), 8.73 (1H, d), 13.08 (1H, s). ^{13}C NMR data (125 MHz, DMSO-d_6, 298 K) δ 111.31, 120.141, 121.926, 122.697, 123.933, 124.638, 134.152, 137.51, 144.40, 148.50, 149.023, 150.83. ESI-TOF MS: m/z 196 $[M+H]^+$.

2.4 Synthesis of dichlorobis(1,10-phenanthroline)ruthenium(II) dihydrate (PC1), dichlorobis(2,2′-bipyridyl)ruthenium(II) dihydrate (PC2) and dichlorobis(2-(pyridin-2-yl)-1*H*-benzimidazolyl)ruthenium(II) dihydrate (PC3)

The precursor complexes **PC1** and **PC2** were synthesized by the procedure reported by Sullivan et al [11]. The complex **PC3** was synthesised by refluxing a mixture of $RuCl_3.3H_2O$ (0.69 g, 2.65 mmol), 2-(pyridin-2-yl)-1*H*-benzimidazole (**P2**) (0.97 g, 5 mmol) and lithium chloride (0.84 g, 20 mmol) in dry DMF (8 mL) with stirring for 12 h under argon atmosphere and cooled to room temperature. Acetone (75 mL) was added to it and kept at 0 °C overnight. The precipitate that separated out was filtered, washed with cold water followed by diethyl ether, dried and recrystallized using DMF. Cis-[Ru(**P2**)$_2$Cl$_2$].2H$_2$O (**PC3)**; Dark violet solid (1.1 g, 69%). ESI-TOF MS: m/z 527 $[M-(Cl+2H_2O)]^+$.

2.5 Synthesis of ligand (L)

To a solution of pyrenylcalix[4]resorcinarene (**P1**) (3.86 g, 3 mmol) and 2-(pyridine-2-yl)-1*H*-benzimidazole (**P2**) (2.34 g, 12 mmol) in 2-methoxyethanol-ethanol mixture (2:1 v/v, 60 mL), an aqueous solution of formaldehyde (37%, 4.50 mL, 150 mmol) was added with stirring under argon atmosphere. After 1 h of stirring at ambient temperature, the reaction mixture was brought to reflux for 48 h. The completion of reaction was checked by thin layer chromatography on silica-gel. The resulting solution was cooled to room temperature and added to ice cold water (600 mL). The precipitate formed was filtered using G3 filter funnel, washed with

methanol (3x20 mL) and dried under vacuum. The red powder obtained was purified using column chromatography by eluting with acetone-hexane (9:1 v/v) solvent mixture and recrystallized using DMF. **L** – Red powder (4.9 g, 77 %), mp >300 °C (dec.). Analytical data (%) found: C, 81.70; H, 4.44; N, 7.99; calculated for $C_{144}H_{92}N_{12}O_8$: C, 81.65; H, 4.38; N, 7.93. ^{1}H NMR data (500 MHz, DMSO-d_6, 298 K) δ 4.77 (8H, s, -*CH*$_2$-), 5.48 (4H, s, -*CH*-), 5.95 (4H, s), 6.30 (4H, s), 6.51 (4H, s), 6.55 (4H, s), 6.68 (4H, s), 6.86 (4H, s), 7.02(4H, s), 7.11 (4H, s), 7.28 (8H, dd), 7.48 (8H, m), 7.71 (4H, dd), 7.98 (8H, ddd), 8.43 (8H, d), 8.69 (4H, d). ESI–TOF MS: m/z 1342 [M-4(**P2**)]$^+$, 1348 [(M+6H)-4(**P2**)]$^+$, 1363 [(M+Na)-4(**P2**)]$^+$.

(Caution: Perchlorate salts are potentially explosive and, therefore, should be handled in small quantities with care.)

2.6 Synthesis of tetranuclear ruthenium(II) complexes of pyrenylcalix[4] resorcinarene, CP1, CP2 and CP3.

A solution of the preformed ligand (**L)** (0.21 g, 0.10 mmol) and $[Ru(phen)_2Cl_2]\cdot 2H_2O$ (0.21 g, 0.4 mmol) or $[Ru(bpy)_2Cl_2]\cdot 2H_2O$ (0.20 g, 0.4 mmol) or $[Ru(\mathbf{P2})_2Cl_2]\cdot 2H_2O$ (0.23 g, 0.4 mmol) in *N*,*N*-dimethylformamide (50 mL) was refluxed with stirring under argon atmosphere for 12 h. The resultant dark red solution was cooled to room temperature and filtered. The volume of the solution was reduced to 5 mL under reduced pressure and 50 ml of aqueous solution of sodium perchlorate was added to it with stirring whereupon a dark red solid separated out. The solid was filtered, washed with water and dried under vacuum. The product was purified by column chromatography on silica eluting with acetone: 0.1 M KNO_3(aq) (9:1 v/v) [12] and recrystallized in hot acetonitrile.

CP1 – Dark red solid (0.37 g, 77 %). Analytical data (%) found: C, 60.81; H, 3.24; N, 8.17; calculated for $C_{240}H_{156}N_{28}O_{40}Cl_8Ru_4$: C, 60.56; H, 3.30; N, 8.24. ^{1}H NMR data (500 MHz, DMSO-d_6, 298 K): δ 5.34 (8H, -*CH*$_2$-), 6.85 (4H, -*CH*-), 7.28 (4H, t), 7.41 (16H, t), 7.62 (8H, d), 7.67 (16H, d), 7.72 (4H, d), 7.77 (4H, m), 7.92 (20H, m), 8.06 (12H, d), 8.18 (12H, d), 8.27 (8H, d), 8.33 (4H, t), 8.39 (8H, d), 8.58 (8H, d), 8.74 (4H, d), 8.80 (8H, d), 9.00 (4H, OH) 9.85 (4H, -*OH*). ESI-TOF MS: m/z 1476.81 [(M-(3ClO_4+2H_2O)]$^{3+}$, 995 [(M+Na)-(4ClO_4+2$C_{16}H_9$+H)]$^{4+}$, 689 [(M-(6ClO_4+H_2O)]$^{6+}$, 656 [(M-(6ClO_4+$C_{16}H_9$+2H_2O)]$^{6+}$, 499 [(M+K)-(8ClO_4+H)]$^{8+}$.

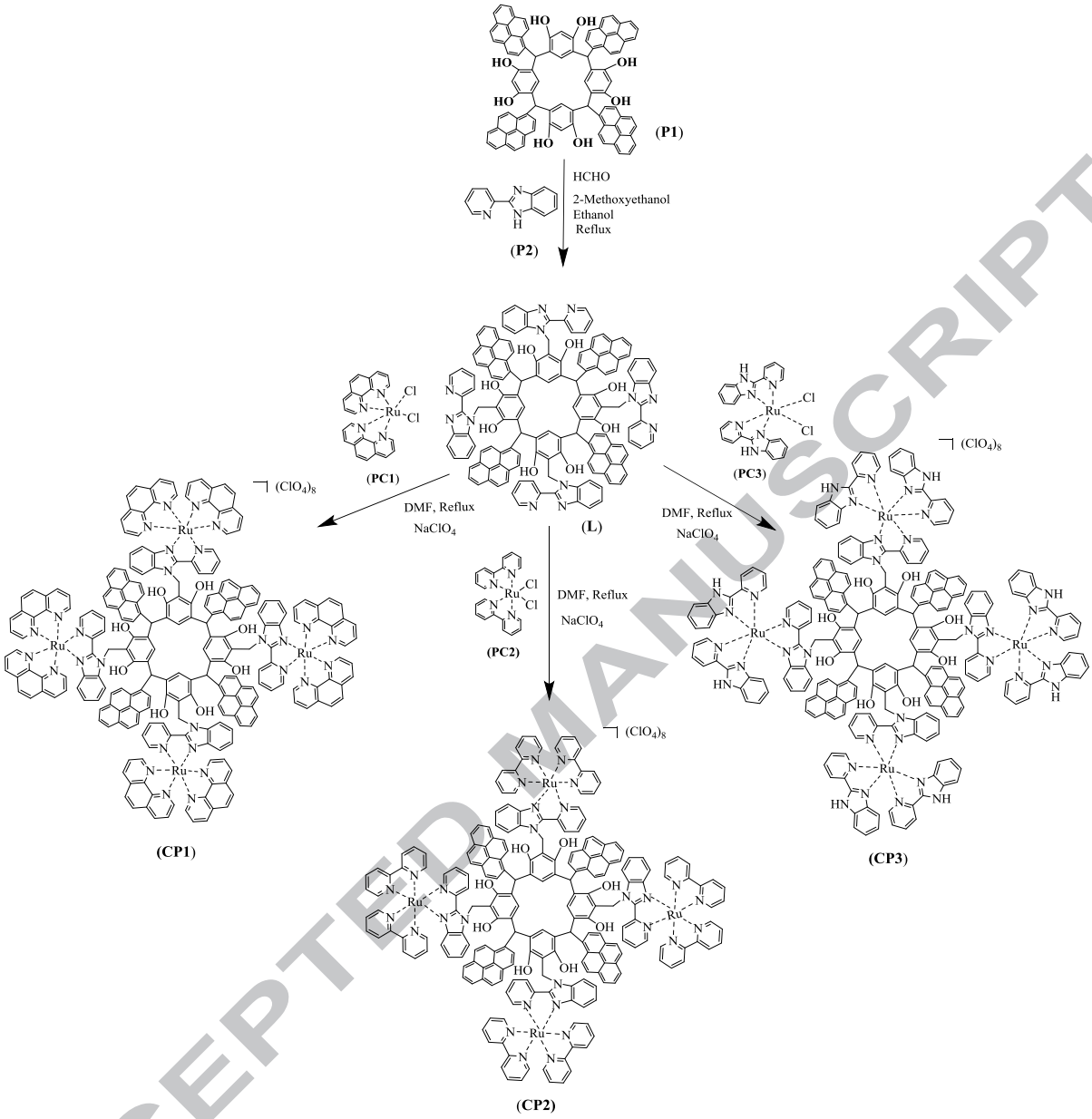

Scheme 1. Synthesis of the ligand (**L**) and tetranuclear ruthenium(II) complexes, **CP1**, **CP2** and **CP3.**

CP2 – Dark red solid (0.33 g, 72%). Analytical data (%) found: C, 58.82; H, 3.34; N, 8.53; calculated for $C_{224}H_{156}N_{28}O_{40}Cl_8Ru_4$: C, 58.90; H, 3.44; N, 8.59. ^{1}H NMR data (500 MHz, DMSO-d_6, 298 K): δ 5.65 (8H, -CH_2-), 6.59 (2H, s) 6.63 (4H, -*CH*-), 7.03(2H, d), 7.36 (16H, s), 7.52 (8H, t), 7.59 (4H, t), 7.71 (4H, d), 7.77(4H, t), 7.85 (16H, m), 7.95 (4H, s), 8.00 (4H, m), 8.08 (4H, m), 8.14 (8H, m), 8.25 (4H, m), 8.33 (4H, m), 8.72 (4H, m), 8.50 (4H, t), 8.55 (12H, d), 8.74 (4H, m), 8.75 (4H, d), 8.83

(16H, d), 9.16 (8H, d), 9.37 (4H, s, -*OH*), 9.42 (4H, s, -*OH*). ESI-TOF MS: m/z 1217 $[(M+5H)-(8ClO_4+7H_2O)]^{3+}$, 1020 $[(M-(4ClO_4+5H_2O)]^{4+}$, 608 $[(M+2H)-8ClO_4+7H_2O)]^{6+}$.

CP3 – Dark red solid (0.39 g, 79 %). Analytical data (%) found: C, 58.91; H, 3.34; N, 10.28; calculated for $C_{240}H_{164}N_{36}O_{40}Cl_8Ru_4$: C, 59.07; H, 3.39; N, 10.33. ^{1}H NMR data (500 MHz, DMSO-d_6, 298 K): δ 5.76 (8H, t), 5.99 (2H, d), 6.05 (4H, d), 6.11 (2H, d), 6.87 (4H), 6.90 (4H, m), 7.05 (12 H, m), 7.10 (16H, m), 7.27 (8H, m), 7.41 (8H, m), 7.52 (4H, m), 7.64 (4H, m), 7.70 (8H, m), 7.86 (4H, m), 7.97 (4H, m), 8.13 (8H, m), 8.23 (4H, m), 8.33 (4H, d), 8.39 (4H, m), 8.45 (4H, m), 8.55 (8H, m). 8.61 (4H, m), 8.67 (4H, m), 8.84 (4H, t), 8.90 (8H, d), 8.50 (4H, d), 9.50 (2H, d, -*OH*), 9.70 (4H, d, -*OH*), 9.85 (2H, d, -*OH*). ESI-TOF MS: m/z 720 $[(M+K)-(6ClO_4+H)]^{6+}$, 686 $[(M+H)-(7ClO_4+H_2O)]^{6+}$, 555 $[(M+H)-(8ClO_4+C_{16}H_9)]^{7+}$, 527 $[(M+K)-7ClO_4]^{8+}$.

3 Results and Discussion

3.1 Synthesis and characterisation of pyrenylcalix[4]resorcinarene (P1)

2,8,14,20-Tetrapyrenyl-4,6,10,12,16,18,22,24-octahydroxycalix[4]resorcinarene **(P1)** was synthesised by the acid catalysed condensation of resorcinol with 1-pyrenecarboxaldehyde (1:1) in refluxing ethanol-water mixture in an inert atmosphere. The ^{1}H NMR spectrum shows resonance signals corresponding to aromatic hydrogen atoms of resorcinol, polynuclear hydrocarbon rings and methine bridge protons. The doublet at 8.9 ppm corresponds to hydroxyl proton of **P1** (Fig. S1). The appearance of doublets indicates that the chemical environment of hydroxyl protons is different. The signal at around 19 ppm in ^{13}C NMR corresponds to the methine bridge formed during condensation reaction (Fig. S2). The ESI-TOF mass spectrum of **P1** shows the molecular ion peak at *m*/*z* 1289 and the peak at *m*/*z* 1312 corresponds to the addition of sodium ion to the molecular ion (Fig. S3).

3.1.1 Crystal structure of pyrenylcalix[4]resorcinarene (P1)

The compound **P1** crystallizes in triclinic crystal system with P$\bar{1}$ space group (Fig. 1). The asymmetric unit of the crystal contains one pyrenylcalix[4]resorcinarene molecule, eight DMF molecules and two water molecules. Two of the DMF molecules are disordered over two positions with a ratio of 54:46 and 50:50, respectively. The molecule adopts a *cis* configuration with rigid boat like conformation and the pyrene rings occupy the axial positions. There are four DMF molecules which are

encapsulated by the resorcinarene molecule and its inversion moiety is linked through strong H-bonds, O(5)-H(5A)...O(10) and O(6)-H(6)…O12. The hydroxyl groups of all resorcinol moieties take part in hydrogen bonding interaction with the amide oxygen of DMF, water and symmetry generated pyrenylcalix[4]resorcinarene molecules, which give rise to three dimensional hydrogen bond network. These solvent mediated interactions stabilize the crystal lattice and the conformation of the molecule (Fig. 2). The hydroxyl groups of upright resorcinol units enhance the intermolecular hydrogen bonds with neighbouring basal resorcinol rings, O(8)-H(8)...O(1). All the hydrogen bonds present in **P1** are given in Table S1. The crystal arrangement is further strengthened by the additional C–H…O and C–H…π interactions. The atoms comprising of C48, C49, C50, C51, C59 and C60 are a part of pyrene ring showing shortest π-π interactions with adjacent pyrene ring involving atoms C58, C67, C69, C70, C71 and C76 with centroid-centroid distance of 3.78 Å and a displacement angle (β) of 24.28°. It also shows a relatively weak π-π interaction with a centroid-centroid distance of 3.85 Å between the other set of pyrene rings (comprising of atoms C32, C33, C34, C35, C43, C44 and C80, C81, C82, C83, C91, C92) with a displacement angle of 18.80°. The dihedral angle between the mean planes of adjacent resorcinol rings is 77.72(0)° and that of adjacent pyrene rings is 14.87(0)°. The pair of resorcinol rings comprising of the basal plane has a dihedral angle of 12.16(0)° while that of the upright resorcinol moieties have a dihedral angle of 24.37(6)°. The complete description of crystal is given in Table 1.

3.2 Synthesis and characterization of 2-(pyridine-2-yl)-1*H*-benzimidazole (P2)

Condensation of equimolar amounts of 2-cyanopyridine and *o*-phenylenediamine in *o*-phosphoric acid followed by neutralization with aqueous ammonia formed **P2**. The ^{1}H NMR spectrum of **P2** in DMSO shows two multiplets, one triplet and three doublets due to the protons present in the benzimidazole and pyridyl rings (Fig. S4). The singlet at 13.1 ppm is assignable to the secondary amine proton of the imidazole ring [13] (Fig. S5). The ESI-TOF mass spectrum shows a peak at *m*/*z* 196 corresponding to the addition of one proton to the molecular ion (Fig. S6).

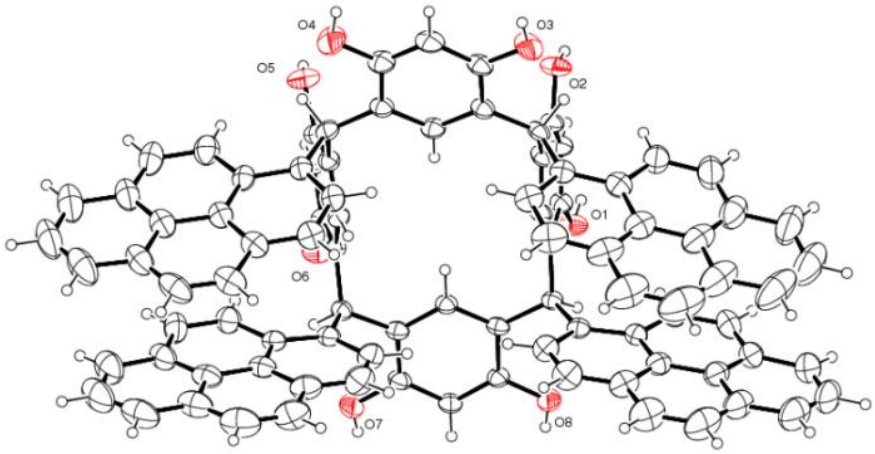

Figure 1. ORTEP representation of **P1** with atoms represented in 40% probability thermal ellipsoids. Solvent molecules are removed for clarity.

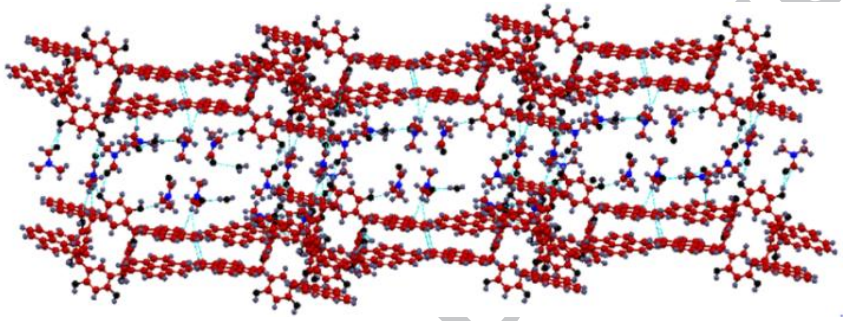

Figure 2. Two dimensional arrangement of **P1** crystal in interaction with the solvent molecules.

3.3 Synthesis and characterisation of ligand L

The benzimidazolyl pyridine functionalised pyrenyl calix[4]resorcinarene (**L**) was synthesized by the aminomethylation of calix[4]resorcinarene (**P1**) with 2-(pyridin-2-yl)-1*H*-benzimidazole (**P2**) and formaldehyde in the refluxing solvent mixture of 2-methoxyethanol and ethanol (2:1 v/v) for 48 h under argon atmosphere (Scheme 1). The product obtained was purified by column chromatography and recrystallized using DMF. The product was characterized using ^{1}H NMR and ESI–TOF mass spectra. The proton nmr spectrum confirms the formation of the ligand by the appearance of a new signal at 4.77 ppm which corresponds to the methylene bridge proton. No signal for hydroxyl groups could be found in the ^{I}H NMR spectrum due to the fast exchange of protons with water molecule (Fig. S8). The ESI-TOF mass spectrum of **L** shows a peak at *m*/*z* 1342 corresponding to the removal of four (2-(pyridin-2-yl)-1*H*-benzimidazole moieties from the molecular ion (Fig. S9).

Table 2. Description of **P1** crystal

Description	
Empirical formula	$C_{116}\ H_{116}\ N_8\ O_{18}$
Formula weight	1910.16
T, K	296(2)
λ, Å	0.71073
Crystal system	Triclinic
Space group	$P\bar{1}$
a,Å	15.7201(7)
b,Å	16.2568(8)
c,Å	22.3882(11)
α, °	76.751(3)
β, °	74.923(3)
γ, °	68.303(3)
V, $Å^3$	5076.4(4)
Z	2
ρ_{calcd}, mg m^{-3}	1.250
Absorption coefficient, mm^{-1}	0.085
F(000)	2024
θ range for data collection, °	2.100 to 25.000
Reflections collected/unique	105029/17818
Absorption correction	Semi-empirical from equivalents
Max. and min. transmission	0.96 and 0.93
Refinement method	Full-matrix least-squares on F^2
Data/restraints/parameters	17818 / 594 / 1401
Goodness of fit on F^2	1.071
Final R indices $[I > 2\sigma(I)]^a$	R1 = 0.0826, wR2 = 0.2067
R indices (all data)[a]	R1 = 0.1702, wR2 = 0.2845
Largest diff.peak and hole	0.757 and -0.430 $eÅ^{-3}$

[a] $R1 = \sum||F_o| - |F_c||/\sum|F_o|$; $wR2 = [\sum\{w(F_o^2 - F_c^2)\}/\sum\{wF_o^2)^2\}]^{1/2}$

3.4 Synthesis and characterisation of complexes, CP1, CP2 and CP3

The reaction of **PC1**, $[Ru(phen)_2Cl_2]$, or **PC2**, $[Ru(bpy)_2Cl_2]$ or **PC3**, $[Ru(\mathbf{P2})_2Cl_2]$ with the preformed ligand **L** in 4:1 molar ratio in refluxing DMF for 12 h followed by the addition of an aqueous solution of sodium perchlorate formed the stable complexes, **CPI**, **CP2** and **CP3**, respectively (Scheme 1). All these complexes were purified by column chromatography and characterized by ^{1}H NMR, UV-visible and ESI-TOF mass spectra. The ^{1}H NMR spectra of these heteroleptic complexes are very complicated due to the non-equivalent phenanthroline, bipyridine and pyridinylbenzimidazole ligand moieties [14]. The ^{1}H NMR spectra of the complexes **CP1**, **CP2** and **CP3** are given in Figs. S11, S14 and S17, respectively. The ESI-TOF mass spectra of complexes show peaks corresponding to the isotopic pattern of ruthenium metal ions {Figs. S12 (**CP1**), S15 (**CP2**) and S18 (**CP3**)}.

3.5 Photophysical studies of the complexes

The electronic absorption spectrum of the free ligand displays bands at λ_{max} 335 and 351 nm assignable to the spin allowed ligand centered (^{1}LC) π–π* transitions due to pyrene moieties. The electronic absorption spectra of the tetranuclear Ru(II) complexes show low energy absorption bands at λ_{max} 439, 456 and 460 nm which could be assignable to the $Ru_{d\pi} \rightarrow$ *phen* or *bpy* or ***P2*** ^{1}MLCT transitions. The higher energy bands at 267, 326 and 342 nm in **CP1**, and at 287, 325 and 340 nm in **CP2** and at 318 in **CP3** are due to the pyridinylbenzimidazole-phenanthroline or -bipyridyl or -pyridinylbenzimidazole interligand π–π* transitions, respectively. The electronic absorption spectrum of ligand is given in Fig. S9 and those of complexes **CP1**, **CP2** and **CP3** are depicted in Figs. S13, S16 and S19, respectively.

The excitation spectrum of the free ligand **L** contains bands at 308 and 355 nm. Upon excitation at 352 nm, the ligand emits at 436 nm in the room temperature (298 K) condition. The emission takes place in the blue end of the visible region due to the pyrene moieties. The emission spectral behaviour of the complexes has been studied at 298 and 77 K in acetonitrile (Fig. 3).

Table 2. Absorption and luminescence spectral data of the complexes

Complex	Absorption, λ_{max} (nm) (ε x 10^{-4}, M^{-1} cm^{-1})	Luminescence						
		298 K					77 K	
		λ_{max} (nm)	Φ_{em} [b]	τ(ns)	K_r [c] $10^4(s^{-1})$	K_{nr} [d] $10^4(s^{-1})$	λ_{max} (nm)	Φ_{em} [b]
CP1	439 (4.16) 342 (10.66) 326 (9.60) 267 (28.86)	579	0.0036	164	2.21	608	568, 605	0.661
CP2	456 (4.56) 340 (13.96) 325 (13.26) 287 (28.76)	607	0.0027	244	1.09	409	612, 652	0.271
CP3	460 (2.95) 318 (32.85)	671	0.0007	95	0.686	1050	657	0.019

[a] Absorption and emission spectra were recorded in CH_3CN at 298 K and in frozen CH_3CN at 77 K. [b] Luminescence quantum yields (Φ) were calculated by integrating the emission profile using $[Ru(bpy)_3]^{2+}$ as the standard (λ_{ex} = 449, λ_{em} = 603). [c] $K_r = \Phi_{em} / \tau$. [d] $K_{nr} = (1/\tau - Kr)$.

The photophysical properties of **CP1**, **CP2** and **CP3** are dependent upon phenathroline, bipyridine and benzimidazolylpyridine ancillary ligands, respectively. It is reported that $[Ru(phen)_3]^{2+}$ and $[Ru(bpy)_3]^{2+}$ complexes show emission bands at 575 and 590 nm, respectively [15] whereas $[(bpy)_2Ru(\mathbf{P2})]^{2+}$ shows emission band at 653 nm [16]. However, phenanthroline-pyridinylbenzimidazole based **CP1** and bipyridine-pyridinylbenzimidazole based **CP2** complexes show emission bands at 579 and 607 nm which are blue shifted in comparison with the parent compound $[(bpy)_2Ru(\mathbf{P2})]^{2+}$. The emission bands of **CP1** and **CP2** at 77 K in frozen CH_3CN are hyperchromic and are observed at higher energy regions of 568 and 605 (sh) nm for **CP1** and at 612 and 652 (sh) nm for **CP2**. The complexes **CP1** and **CP2** show higher emission intensity in comparison with complex **CP3** due to the effective energy transfer of light emitting sensitizers phenanthroline and bypyridine, respectively. The emission from **CP3** is found to be weak as that of its mononuclear $[Ru(\mathbf{P2})_3]^{2+}$ complex [17]. However the same at 77 K in frozen CH_3CN is hypsochromically shifted to 657 nm with 75 fold increase in the emission intensity. The effective overlapping of the emission band of the pyrene appended ligand (**L**) with the absorption band of complexes warrants energy transfer between the pyrene moiety and Ru(II)

(phen/bpy/**P2**) complexes, **CP1**, **CP2** and **CP3**, respectively. The low emission intensity of **CP3** can be substantiated with high value of nonradiative decay constant which may be due to the deprotonation of pyridinylbenzimidazole ancillary ligand. At 77 K all the complexes show hyperchromic effect and the emission maxima exhibit blue shift due to rigidochromic effect which is the characteristics of MLCT emitters [18]. As the temperature is lowered the rigidochromic effects vary in heteroleptic ligands since different excited states display different changes in charge distribution. This can possibly lead to a switching of the lowest excited state with another excited state or states close in energy to it. In intermediate regions, when the energy of each of the switching states is identical then two emissions may be observed. This may be the reason for the presence of shoulders for the emission maxima at 605 and 652 nm for **CP1** and **CP2**, respectively at 77 K [19]. The complexes show single exponential lifetime decay at 298 K.

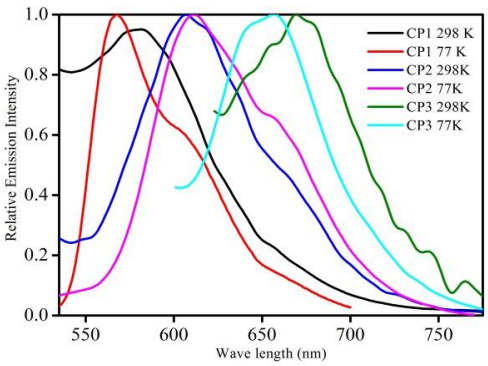

Figure 3. Combined emission spectra of **CP1**, **CP2** and **CP3** at 298 and 77 K.

The emission life time of the complexes decreases in the order **CP2**>**CP1**>**CP3** with the values of 244, 164 and 95 ns in the solution which can be substantiated by concomitant increase in nonradioactive decay rate constant, proving an effective nonradiative pathway in **CP3**. The quantum yield of the complexes increases considerably when recorded at 77 K in all the complexes than the same at 298 K which could be attributed to the lowering of nonradiative decay path ways [20]. The emission profile and emission maxima of the complexes are independent of the excitation wavelength. Relative to the solution spectra, the emission spectra in frozen glass are sharper and exhibit hyperchromic effects [21]. Table 2 summarizes the emission maxima, quantum yields and luminescence lifetimes of the ruthenium complexes.

3.6 Electrochemical study of the complexes

The redox behaviour of the ruthenium metal ion in the complexes, **CP1**, **CP2** and **CP3** was investigated using cyclic voltammetry. The cyclic voltammograms (Figs. S20a, S21a and S22a) of all the complexes show metal centered redox peaks in the positive potentials and ligand centered redox peaks (Figs. S20b, S21b and S22b) in the negative potentials [18]. In **CP1**, **CP2** and **CP3**, $E_{1/2}$ values for Ru(II)/Ru(III) redox couple are measured as 1.06, 1.05 and 0.98 V vs Ag/Ag^{+}, respectively. The low $E_{1/2}$ value for Ru(II)/Ru(III) redox couple in **CP3** may be attributed to the deprotonatation in benzimidazole moiety followed by increase in electron density over the ligand. The ΔE_p values for Ru(II)/Ru(III) redox couples of **CP1**, **CP2** and **CP3** are found to be 80, 70 and 70 mV and their i_{pa}/i_{pc} ratios are calculated as 0.79, 0.51 and 0.50, respectively. These indicate that the redox processes are quasireversible and may be that all four independent one-electron metal centered redox processes take place simultaneously in the complexes. The complexes **CP1**, **CP2** and **CP3** show irreversible waves at -0.88, -0.89 and -0.78 V, respectively for the ligand centered redox processes.

4 Conclusions

A new synthetic strategy has been developed to functionalise the ortho position of resorcinol moieties in calix[4]resorcinarene using pyridinylbenzimidazole. The present work opens a new era in the resorcinarene chemistry for the synthesis of molecular container compounds or cavitands. The synthesis of benzimidazolyl pyridine functionalised pyrenylcalix[4]resorcinarene and its tetranuclear ruthenium(II) complexes containing bidentate ancillary ligands offers a wide scope for the construction of a plethora of transition metal complexes on the upper rim of resorcinarene. Despite the bigger size of the ligand, the complexes are soluble in acetonitrile making them favourable for a detailed photophysical and electrochemical studies. The spin allowed ligand centered π-π^* transition of pyrene moieties and the ^{1}MLCT transitions due to ruthenium polypyridyl complexes overlap with each other paving way for effective energy transfer processes within one multicomponent system. The luminescence spectra of the complexes at 77 K show increase in luminescence emission intensity as compared to the emission at 298 K showing promising candidature of the complexes for fluorescence studies. An enhanced increase in quantum yields of the complexes with improved photophysical properties provides options for the development of new aminomethylated calix[4]resorcinarene based

ruthenium complexes quite suitable to be used as biomarkers. The electrochemical properties, showing quasireversible nature of the Ru(II)/Ru(III) redox systems, give nod for understanding possible similar redox properties to be evolved from Fe based calix[4]resorcinarenes to be used in biological systems. Therefore, these ruthenium complexes with new ligand modification may be useful in designing photoresponsive molecular receptors for photodynamic therapy and sensing study.

Acknowledgements

The authors express their gratitude to Dr. Babu Varghese and Dr. P. K. Sudadevi Antharjanam, SAIF, IIT-Madras, Chennai, India for their help in solving crystal structure. The authors gratefully acknowledge the services of SAIF, IIT-Madras, Chennai for NMR spectra; SAIF, Punjab University, Chandigarh for ESI-MS; and NCUFP, University of Madras, Chennai for the emission lifetime measurements.

Appendix A. Supplementary data.

Crystallographic data of **P1** (PYRSC) was deposited with the Cambridge Crystallographic Data centre, CCDC# 1446135. The data can be obtained free of charge via www.ccdc.cam.ac.uk/data_request/cif.

References

1 (a) A. G. S. Hogberg, *J. Org. Chem.* 45 (1980) 4498-4500. (b) P. Timmerman, W. Verboom and D. N. Reinhoudt, *Tetrahedron* 52 (1996) 2663-2704. (c) X. Han, B-B. Lu, J. Yang, H. Wu, Y-Y. Liu and J-F. Ma, *Inorg. Chim. Acta* 482 (2018) 579- 587. (d) S. A. Senthan and V. Alexander, *Dalton Trans.* 44 (2015) 14813-14822.

2 (a) O. Lukin, A. Shivanyuk, V. V. Pirozhenko, I. F. Tsymbal and V. I. Kalchenko, *J. Org. Chem.* 63 (1998) 9510-9516. (b) R. Puttreddy, N. K. Beyeh and K. Rissanen, *Cryst. Eng. Comm*. 18 (2016) 4971-4976. (c) S. Rat, J. Gout, O. Bistri and O. Reinaud, *Org. Biomol. Chem.* 13 (2015) 3194-3197.

3 M. Pietraszkiewicz, O. Pietraszkiewicz, E. Uzig, P. Prus, Z. Brzózka, K. Woźniak, R. Bilewicz, T. Borowiak, and M. Mączyñski, *Butlerov Communications* 3 (2000) 55-65.

4 J. Han and C. Yan, *J. Incl. Phenom. Macrocycl. Chem.* 61 (2008) 119-126.

5 (a) D. J. Cram, S. Karbach, H. E. Kim, C. B. Knobler, E. F. Maverick, J. L. Ericson and R. C. Helgeson, *J. Am. Chem. Soc*. 110 (1988) 2229-2237. (b) X. Han, J. Park, W. Wu, A. Malagon, L. Wang, E. Vargas, A. Wikaramanayake, K.N. Houk and R.M.

Leblanc, *Curr. Opin. Biotechnol.* 34 (2015) 41-47. (c) D. A. Leigh, P. Linnane, R. G. Pritchard and G. Jackson, *J. Chem. Soc. Chem. Commun.* 4 (1994) 389-390. (d) Y. Matsushita and T. Matsui, *Tetrahedron Lett.* 34 (1993) 7433-7436.

6 (a) B, N. Bideh, C. Roldan-Carmona, H. Shahroosvand and M. K. Nazeeruddin, *Dalton Trans.* 45 (2016) 7195-7199. (b) M. Kuss-Petermann and O. S.Wenger, *J. Am. Chem. Soc*. 138 (2016) 1349-1358.

7 (a) D. Maity, C. Bhaumik, D. Mondal and S. Baitalik, *Inorg. Chem.* 52 (2013) 13941-13955. (b) S. Mandal, V. Kundi, D. K. Seth, K. Srikanth and P. Gupta, *Polyhedron* 80 (2014) 290-297.

8 H. Ishida, S. Tobita, Y. Hasegawa, R. Katoh and K. Nozaki, *Coord. Chem. Rev.* 254 (2010) 2449-2458.

9 J. R. Lakowicz, *Principles of Luminescence Spectroscopy, 3rd ed*.; Springer, New York, 2006.

10 A.W. Addison and P.J. Burke, *J. Heterocycl. Chem*. 18 (1981) 803-805.

11 B. P. Sullivan, D.J. Salmon and T.J. Meyer, *Inorg. Chem*. 17 (1978) 3334-3341.

12 (a) V. Balzani, A. Juris, and M. Venturi, *Chem. Rev.* 96 (1996) 759-833. (b) Q. Cheng, Y. Cui, N. Xiao, J. Lu, and C.-J. Fang, *Molecules* 23 (2018) 1649-1659. (c) S. L. Dabb and N. C. Fletcher, *Dalton. Trans.* 44 (2015) 4406.

13 M. M. H. Khalil, S. A. Ali and R. M. Ramadan, *Spectrochim. Acta A.* 57 (2001) 1017-1024.

14 E. T. Luis, G. E. Ball, A. Gilbert, H. Iranmanesh, C. W. Newdick and J. E. Beves, *J. Coord. Chem.*, 69 (2016) 1686-1694.

15 D. M. Klassen and G. A. Crosby, *J. Chem. Phys.* 48 (1968) 1853-1858.

16 Yi. Hunan, A. C. Joe and T.S. I. John, *Dalton. trans.* (2003) 685-691.

17 M. R. McDevitt, Y. Ru and A. W. Addison, *Transition Met. Chem*. 18 (1993) 197-204.

18 (a) R. J. Watts and D. Missimer, *J. Am. Chem. Soc*.100 (1978) 5350-5357. (b) A. A. Viveke and V. Alexander, *RSC Adv*. 4 (2014) 44269-44273

19 T. J. Meyer, *Pure and Appl Chem*. 58 (1986) 1193-1206.

20 A. Juris and V. Balzani, *Coord. Chem. Rev*. 84 (1988) 85-277.

21 S. Baitalik, U. Flörke and K. Nag, *Inorg. Chem.* 38 (1999) 3296–3308.

Graphical abstract

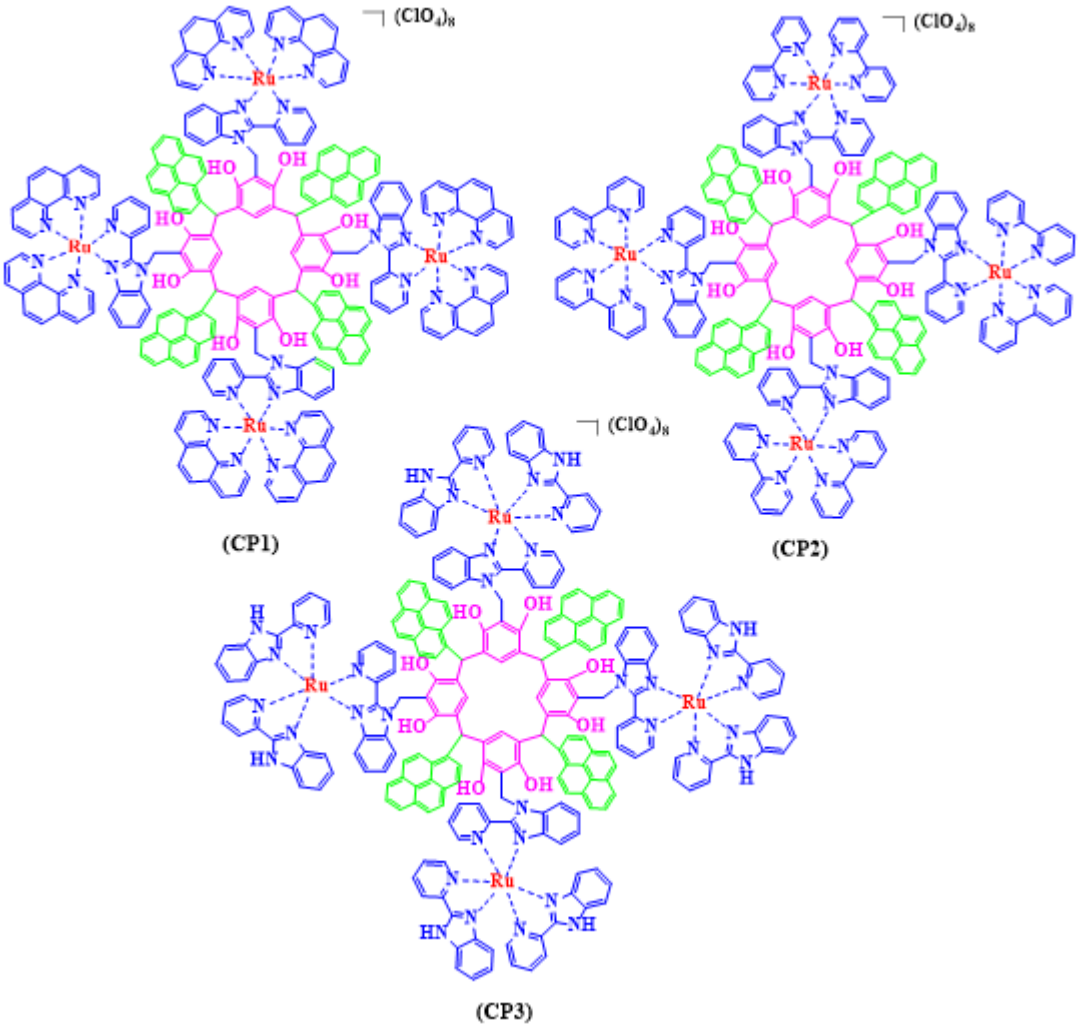

Highlights

- A new pyrenylcalix[4]resorcinarene (**P1**) was synthesised and structurally characterised using single crystal X-ray diffraction technique.
- A novel benzimidazolyl functionalised pyrenylcalix[4]resorcinarene ligand (**L**) was synthesised.
- Tetranuclear Ru(II) complexes of the ligand, **CP1**, **CP2** and **CP3** were prepared and spectroscopically characterised.
- Luminescence and electrochemical studies of the complexes have been performed.
-